

# Vacuum Circuit Breakers in Flexible AC Transmission Systems

Timo Wenzel and Thomas Leibfried, *Member, IEEE*

**Abstract**—This paper shows two applications for using vacuum circuit breakers (VCBs) in flexible ac transmission systems in the high-voltage (HV) power grid. This is first a mechanically switched reactor, which is series connected to a thyristor-controlled series compensator in order to enhance the inductive working range. Nevertheless, the switching frequency of VCBs is limited by their mechanical properties. In order to achieve a higher switching frequency, more VCBs are switched in parallel to each other. Second, a device is investigated, which consists of mechanically switched capacitors and a mechanically switched reactor. It is connected to a node in the HV system in order to enhance the voltage quality and to avoid a voltage collapse. Since VCBs are mainly available in the medium-voltage range, a transformer is used to connect the mechanically switched device to the HV system. In this paper, it could be shown that the mechanically switched series reactor is able to enhance the damping progress of power oscillations and that the mechanically switched device using VCBs can stabilize the voltage of the node in case of disturbances, such as faults in the power system. Furthermore, the electrical stress on the VCBs has been assessed for different simulation cases with PSCAD.

**Index Terms**—Flexible ac transmission systems (FACTS), load flow, power system stability, PSCAD, vacuum circuit breakers (VCBs), voltage control.

## NOMENCLATURE

FACTS	Flexible ac transmission systems.
MSC	Mechanically switched capacitor.
MSD	Mechanically switched device.
MSR	Mechanically switched reactor.
MSSR	Mechanically switched series reactor.
POD	Power oscillation damping.
TCSC	Thyristor-controlled series compensator.
TRV	Transient recovery voltage.
VCB	Vacuum circuit breaker.

## I. INTRODUCTION

**F**LEXIBLE ac transmission systems (FACTS) are used to increase the transmission capacity and stability of transmission networks and stabilize the voltage at load nodes.

Manuscript received April 11, 2011; revised September 10, 2011; accepted October 12, 2011. Date of publication November 30, 2011; date of current version December 23, 2011. Paper no. TPWRD-00283-2011.

The authors are with the Institute of Electric Energy Systems and High-Voltage Technology, Karlsruhe Institute of Technology, Karlsruhe 76131, Germany (e-mail: timo.wenzel@kit.edu; thomas.leibfried@kit.edu).

Color versions of one or more of the figures in this paper are available online at <http://ieeexplore.ieee.org>.

Digital Object Identifier 10.1109/TPWRD.2011.2172820

Usually, they are equipped with power semiconductors (e.g., thyristors) which allows them to become effective within some milliseconds. This paper investigates the possibilities of using vacuum circuit breakers (VCBs) instead of the power semiconductors due to economical reasons. At least for some applications, VCBs are more cost efficient as the semiconductors including their additional components, such as triggering and cooling [1]. They are mainly available in the medium-voltage (MV) range up to 40.5 kV.

The utilization of VCBs in FACTS is investigated for two applications as follows.

- 1) A mechanically switched series reactor (MSSR) is series connected to a TCSC. The reactor can be periodically short-circuited by VCBs with a special configuration. The combination of MSSR and TCSC can be used for power oscillation damping.
- 2) A mechanically switched device (MSD) consisting of capacitors and a reactor can be connected to a load node in order to stabilize the voltage.

An MSSR has been investigated before, but mostly for short-circuit limitation [2], [3] or for power-flow control [4], [5] and with other types of circuit breakers and power grids with lower voltage levels.

A self-provided VCB model considering the electrical characteristics of VCBs is used to investigate the electrical stress (e.g., overvoltages) while the VCBs are switching.

### A. Power Oscillations

Power oscillations may occur in electrical power systems after disturbances, such as line faults or substation blackouts. Generally, they are damped by the damper windings of the synchronous generators and by power system stabilizers but, in some cases, this kind of damping is insufficient [6]. Another possibility is that the power system stabilizers are not well coordinated with each other in the power grid, so that an undamped oscillation can result [7]. Additional damping is then necessary in order to return into a stable operation point.

### B. Mechanically Switched Series Reactor (MSSR) and TCSC

Normally, a TCSC is used for power oscillation damping (POD) in extensive transmission systems. While damping a power oscillation, the TCSC runs mainly in the capacitive range because the thyristor currents reach undesired high values in the inductive range [8], [9]. The idea is to enhance the inductive working range with the MSSR using VCBs in a special configuration presented in Section II-A. For damping a power oscillation, the TCSC has to work in the maximum capacitive range immediately after a fault. When the maximum value of the power oscillation is reached, the MSSR has to

be inserted into the line and the capacitive reactance of the TCSC has to be minimized. At minimum power oscillation, the MSSR has to be removed again and the capacitive reactance of the TCSC has to be increased. This can be repeated until the power oscillation is damped sufficiently. The maximum power oscillation frequency investigated in this paper is 1 Hz, so the MSSR has to be switched every 0.5 s. In steady-state operation of the power system, it remains short-circuited.

### C. Mechanically Switched Device (MSD)

Usually, static var compensators (SVCs) are used to stabilize the voltage at a load node in the power system and to improve the power factor of the connected load. The new idea is to create a device which is mechanically switched by VCBs and to investigate its possibilities in an electric energy system. It consists of mechanically switched capacitors (MSCs) and a mechanically switched reactor (MSR) and is connected to the HV system by a transformer. A special point of interest in this paper is if the MSCs can avoid voltage instability when the load consists of several induction machines: If the voltage at the load node breaks down because of faults or line outages, the induction machines decelerate which leads to a higher consumption of reactive power. This, in turn, leads to a further reduction of the voltage at the node. If the duration of the fault exceeds a certain limit, the mechanical shaft torque of the machines gets higher than the electrical torque, thus making it impossible to recover rated speed [10]. The voltage instability then occurs in the form of a progressive gradual fall of the voltage at the respective node [11]. A possibility to break this loop is to offer capacitive reactive power directly at the involved node in order to boost the voltage. The machines can reaccelerate and obtain their rated speed. The MSD is described in Section II-C.

## II. SYSTEM DESIGN

### A. VCBs

VCBs are mainly available in the MV range [12]. The VCBs selected in this investigation have a rated voltage of 36 kV and a rated current of 2.5 kA [13]. Their short-duration power-frequency withstand voltage is 96 kV. This value is used as the maximum voltage capability of the VCB model. The tubes need maintenance after 30 000 switching operations, with the mechanical parts needing maintenance after 10 000 switching operations [14]. Considering the expected number of switching operations and the voltage and current requirements, this type of breaker seems to be adequate.

The VCBs used in case of the investigation with the MSSR have a special operating mechanism and are able to switch with a frequency of 0.5 Hz. Since one VCB of this kind is too slow to damp a power oscillation with a maximum frequency of 1 Hz, four VCBs are used. There are two branches connected in parallel to the reactor. Two series-connected VCBs as can be seen in Fig. 1 are in both branches.

Fig. 2 shows the switching status of the VCB configuration in order to insert and remove the reactor into the controlled line with a frequency of 1 Hz. The minimum time between status changes of each VCB is 1.5 s since three cycles have to pass by.

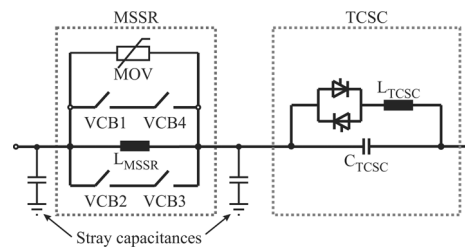


Fig. 1. MSSR and TCSC configuration.

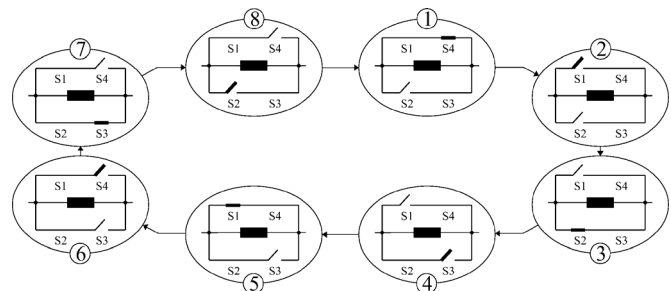


Fig. 2. Switching status of the VCB configuration.

It should be mentioned that VCBs have an on- and off-delay time. The on-delay time is the time from closing command to closed contacts and the off-delay time from opening command to the start of movement of the contacts. In case of this investigation, both delay times are set to a constant value of 45 ms according to [14]. Since this delay time is short compared to the period of one power swing, a negative influence on the damping performance is not expected.

Vacuum has fast recovery strength after arc interruption at current zero [15]. This is important concerning the investigation with the MSD: The VCB-voltage rises to the double value of the steady-state voltage amplitude while disconnecting a capacitor from a voltage source within half a period of power frequency. The VCBs used in this investigation can handle capacitive currents up to 70% of their rated current. The maximum current amplitude when closing a capacitive circuit should be limited to 10 kA for the used VCB [13]. But according to the standards [16], every VCB has to withstand an inrush current with an amplitude of 20 kA at a maximum frequency of 4.2 kHz while switching a capacitor. This value is taken as the maximum current amplitude while closing a capacitive circuit.

### B. Design of the MSSR and TCSC

The MSSR and TCSC configuration is shown in Fig. 1. The reactor of the MSSR can be periodically short-circuited by the four VCBs as described in the previous section. The TCSC can be seen on the right side. A POD controller is used to assign a reactance for the combination of MSSR and TCSC. Local signals, such as the active power, bus voltage, or bus current are preferable as the input signal [17], so the active power is chosen as the input signal. In case of a short circuit in the electrical network while the MSSR is inserted, the opened VCBs are stressed with high voltages as the short-circuit current flowing through the reactor of the MSSR causes an HV drop across it. Hence, a protective circuit has to be installed. A metal-oxide varistor (MOV) switched in parallel to the reactor can serve this purpose, see

TABLE I  
VOLTAGE AND REACTIVE POWER OF THE MSD, CURRENTS OF THE MSCs/MSR, VOLTAGE ON THE HV SIDE 400 kV

No. of MSCs/MSR	$V_{MSD}$ (rms, low voltage side) in kV	reactive power in Mvar	current (per MSC) in kA	current (MSR) in kA
0/1	33.4	45	–	0.74
1/1	34.7	-45	1.56	0.76
1/0	35.4	-91	1.59	–
2/1	36.2	-141	1.63	0.79
2/0	36.9	-191	1.65	–
3/1	37.7	-246	1.69	0.82
3/0	38.5	-300	1.72	–

Fig. 1. The MOV protects the device as soon as the maximum voltage is exceeded while the short-circuit current flows. The command to close the parallel VCB is immediately given when the short circuit is detected. Once the short circuit is removed, the VCB opens and the MSSR is utilizable for POD again. The MOV can meanwhile cool down. If the MSSR is short-circuited by the VCBs before a fault, which is the case in steady-state operation of the electrical system, no problem is expected, because the VCBs can handle short-circuit currents up to 40 kA [14].

### C. Design of the MSD

The MSD consists of MSCs and an MSR. The purpose is to achieve a capacitor bank with a preferably high reactive power. In this investigation, the deliverable capacitive reactive power is chosen to be 300 Mvar. In order to have a grading, the total capacitance is split into three individual parts with the same ratings. The MSR has approximately half of the reactive power of one MSC in order to achieve finer reactive power graduation. The low-voltage side of the transformer used to connect the MSCs/MSR to the HV node is set to 34 kV. This is slightly smaller than the rated voltage of the used VCBs in order to achieve a higher safety margin.

Two types of capacitor switching are possible: single-bank switching and back-to-back switching. In case of single-bank switching, only one capacitor is connected to the grid. The inrush current is mainly affected by the inductances on the path from the source to the capacitor. In case of back-to-back switching, where one capacitor is already connected to the grid, and another one is connected afterwards, the inrush currents are mainly influenced by the inductances in the path from the first to the second capacitor. Current limiting reactors are installed in order to reduce the currents in case of back-to-back switching. It should be mentioned that the transformer and the current-limiting reactors consume a part of the capacitive reactive power. This is incorporated when the capacitor ratings are assigned. A load-flow calculation results in a value of  $C = 172 \mu\text{F}$  for each MSC. A star connection with an ungrounded neutral point is used. The MSR has an inductance of  $L = 70 \text{ mH}$ .

Table I shows the voltage on the low-voltage side of the transformer, the reactive power, and the current for different combinations of MSCs/MSR.

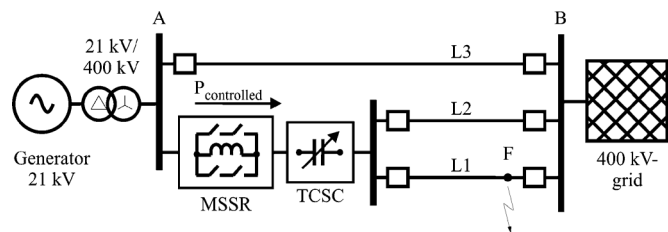


Fig. 3. MSSR and TCSC—Electric network configuration.

The capacitive voltage rise due to the increasing number of connected capacitors can be seen in column 2. The steady-state currents are all within the specifications of the used VCB.

The current-limiting reactors are designed to the fourth harmonic together with the capacitances of the MSCs: Choosing a smaller resonant frequency would decrease the expected inrush currents but it is not advisable in order to retain a safety margin to the power system frequency. Theoretically, the maximum voltage amplitude across the switching element is 2.5 times the amplitude of the steady-state system voltage when ungrounded capacitors and an ungrounded low-voltage side of the transformer are used. It can be calculated by the following equation [18]:

$$\hat{U}_{VCB} = 2.5 \cdot \frac{\sqrt{2}}{\sqrt{3}} \cdot V_{MSD\_rms}. \quad (1)$$

Regarding the capacitive voltage rise and assuming that all three MSCs are connected, a maximum voltage amplitude of  $38.5 \text{ kV} \cdot \sqrt{2}/\sqrt{3} \cdot 2.5 \approx 78.6 \text{ kV}$  is expected, which is within the rated short-duration power-frequency withstand voltage.

### III. SIMULATION MODEL

The simulation tool used is PSCAD, which is a graphical interface to the EMTDC software [19].

#### A. MSSR and TCSC—Electric Network Configuration

An electric network with a line-line voltage of 400 kV and a system frequency of 60 Hz is investigated in this study. A generator is connected to a 400-kV grid by three parallel transmission lines. Lines 1 and 2 have the same length of 125 km each. Line 3 represents a parallel corridor with a length of 150 km. The lines are modeled by a distributed RLC traveling-wave model which is offered in PSCAD [19]. A Donau pylon [18] tower model is used. The corresponding PI-section model line impedance can be calculated to  $0.3 \Omega/\text{km}$ . Fig. 3 shows the electrical configuration.

The 400-kV grid is represented by a strong node with a short-circuit power of 100 GVA. The X/R-Ratio of the source impedance is 10. Therefore, the impedance of this supply is  $X_s = 1.6 \Omega \cdot \exp(j 84.24^\circ)$ .

The synchronous generator symbol represents four machines with 700 MVA each. The rated voltage of every generator is 21 kV, and the inertia constant is  $H = 5 \text{ s}$ . The parameters influencing the frequency of the power oscillation are the inertia constant, the voltage level, the impedance of the transmission system, and the stationary load angle before the fault [20]. For a

TABLE II  
EIGENVALUES AND DAMPING RATIO

line outage	real part $\sigma$	imaginary part $\omega$	frequency $f$ (in Hz)	damping ratio $\zeta$
–	-0,1297	$\pm 6,3977$	1,0182	0,020
L 1	-0,0290	$\pm 5,6948$	0,9064	0,005
L 3	-0,0767	$\pm 6,0231$	0,9586	0,013

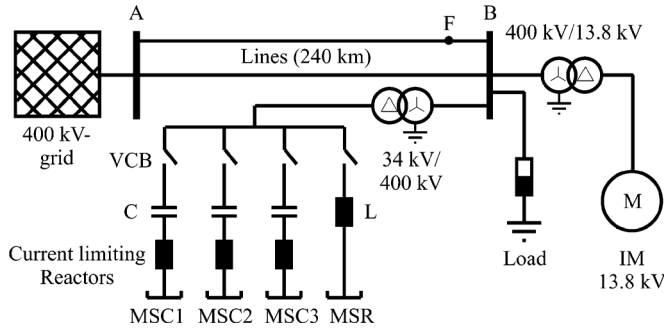


Fig. 4. MSD—Electric network configuration.

single-machine infinite bus (SMIB) system, there is one natural frequency. But a change in the grid configuration like an outage of a power line also causes a change in the power oscillation frequency. The respective values are given in Table II.

The combination of MSSR and TCSC is placed at station A (see Fig. 3) and controls the active power  $P_{\text{controlled}}$  over lines 1 and 2. The degree of compensation of the TCSC is set to approximately 8% of line 1 or 2 and the inductance of the MSSR is 20 mH. The TCSC is working at the lowest capacitive reactance in steady state which is 3  $\Omega$ . The TCSC capacitance is 875  $\mu\text{F}$  and the TCSC inductance is 1.26 mH. The maximum achievable capacitive reactance of the TCSC is three times the steady-state value at a control angle of approximately 147.5°. The MSSR has a reactance of 7.5  $\Omega$  reduced to 4.5  $\Omega$  by the reactance of the TCSC in steady state. The quality factor of the MSSR reactor is set to 180 so a series resistor with 42 m $\Omega$  is considered in every phase. Two stray capacitances with a value of 100 pF are considered at the terminals of the MSSR.

In the base scenario, the generators transmit 2258 MW into the grid. Lines 1 and 2 are loaded by 830.5 MW each and line 3 by 585 MW. The maximum current of the MSSR is limited to 2.5 kA due to the ratings of the VCBs. In the base scenario, it is 2.45 kA. A fault can be applied at point F (see Fig. 3). All simulated cases together with further parameters are mentioned in Section IV.

### B. MSD—Electric Network Configuration

The line-line voltage of the investigated electric network is again 400 kV with a system frequency of 60 Hz. Fig. 4 shows the electrical configuration.

A load is connected to the grid by two parallel transmission lines with a length of 240 km each. The short-circuit power of the source is 100 GVA like in the previous electrical network configuration. The same line model is used here too.

The load content is a combination of a load with a specific load characteristic and a contingent of induction machines. The

load consumes altogether an active power of 1000 MW. The induction machine symbol represents 300 machines, whereas each motor consumes an active power of approximately 2.33 MW. The rated voltage of the motors is 13.8 kV so a transformer connects them to the HV system. The transformer has a rated apparent power of 1000 MVA. The inertia constant of the induction machines is set to  $H = 0.75$  s. It has been calculated from the data of an induction machine with an active power of 1.9 MW [21] and has a huge impact on the loss of speed of the machines in case of voltage drops at their terminals. The dependency between the mechanical shaft load and the machine speed can be chosen by changing the exponent of the motor mechanical torque from zero (conveyor system) to two (fans or pumps). The higher the exponent is, the more stable the machines behave in case of voltage drops.

Two scenarios are investigated as follows.

Scenario a: A voltage-varying time-independent load characteristic with a 0.9 power factor is used. A constant current characteristic is assumed for the active power and a constant impedance characteristic is for the reactive power. This represents a typical load characteristic [20].

Scenario b: The load consists of 70% induction machines and an additional 30% of the load described before. It is a typical contingent of induction machines in electric power systems [20].

The load can be increased or decreased in order to produce a voltage drop or a voltage rise in scenario a. The voltage can be varied from 376 kV to 408 kV in 4-kV steps by changing the load correspondingly.

The three MSCs and the MSR shall compensate the voltage deviation and are connected in parallel to the load by a transformer with a rated power of 300 MVA. One MSC increases the voltage by 8 kV, the MSR decreases it by 4 kV. The LV side of the transformer is in delta connection. An additional bus inductance of 20  $\mu\text{H}$  is incorporated in every MSC/MSR. Stray capacitances with 75  $\mu\text{F}$  to ground are considered at each terminal of the MSR. The current-limiting reactors and the reactor of the MSR have a quality factor of 180, so a resistance is series connected to them. A discharging resistor with approximately 103 k $\Omega$  is incorporated for each MSC. This leads to a discharging time constant of 18 s. A stray capacitance of 100 pF is incorporated across all VCB contacts.

### C. VCB Configuration

The VCB model used in this investigation has been described in [22] where it was used to simulate a vacuum contactor. However, it can be used for modelling a VCB with new parameters, which are given in Table III.

The maximum voltage of the considered VCB is taken from [14]. The arc voltage is within the range of 20 to 30 V [12] and can be neglected in case of this investigation. It is only required if energy conversion in the tube has to be considered. The chopping current is set to a constant value of 5 A differing from [22]: The simulation results are better comparable and it represents the worst case scenario, as typical values of VCB chopping currents lie in the range of 2 to 5 A [12], [13]. The values of the dielectric strength/recovery slope are estimated.

TABLE III  
SETUP PARAMETERS OF THE VCB MODEL

Parameter	Value
maximum voltage	96 kV
Resistance (open)	1000 M $\Omega$
Resistance (closed)	80 $\mu\Omega$
slope of dielectric strength	5 kV/ $\mu$ s
slope of dielectric recovery	15 kV/ms

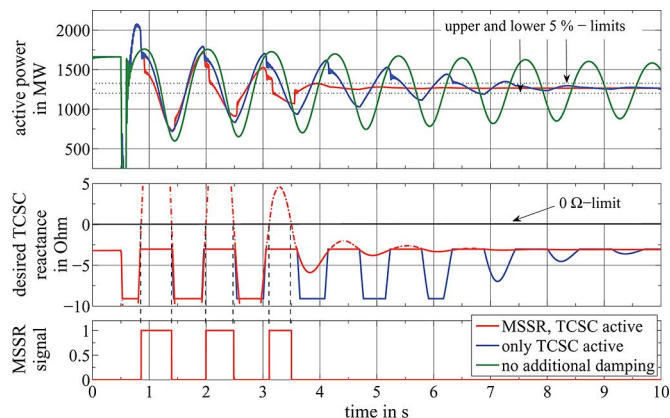


Fig. 5. POD in comparison:  $L_{MSSR} = 20$  mH,  $C_{TCSC} = 875$   $\mu$ F,  $L_{TCSC} = 1, 26$  mH,  $X_{TCSC} = 3 \dots 9\Omega$ ,  $X_{MSSR} = 7, 5 \Omega$ .

#### IV. SIMULATION RESULTS

In PSCAD, a constant integration time-step size must be used for the entire simulation. The largest time step used for any of the simulations is 10  $\mu$ s. The simulations requiring more detail used a 1- $\mu$ s time step.

##### A. MSSR and TCSC

The time until an occurring power oscillation has decayed is assessed for three different cases in the base scenario as follows.

- Case 1) The MSSR and the TCSC are both in service.
- Case 2) Only the TCSC is in service.
- Case 3) No additional damping is delivered.

The results are shown in Fig. 5.

A grounded three-phase fault is applied at point F (Fig. 3) and after 80 ms, it is removed by tripping line 1. The active power in line 2 after the fault is 1264 MW. The upper graph of Fig. 5 shows the transmitted active power  $P_{controlled}$ . The upper and lower 5% limits are given by the dashed lines. The middle graph of Fig. 5 shows the desired reactance of the TCSC, which is limited to the capacitive range. The dashed line in the middle graph shows the total desired reactance for the combination of MSSR and TCSC. The reactor of the MSSR is inserted every time the 0- $\Omega$  limit is exceeded, three times in the given case. The lower graph of Fig. 5 shows the switching command of the MSSR. It can be seen in the upper graph that the power oscillation decays much faster if the TCSC and the MSSR are in service. The peak-peak amplitude of the oscillation reaches within the 5% limits after 40 s without additional damping. If only the TCSC is active, the oscillation needs approximately 6.8 s to get into the 5% range. If both elements are active, it

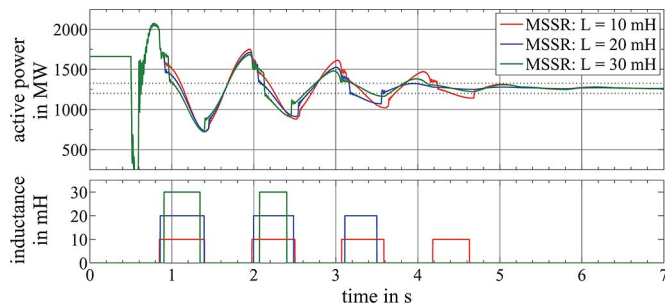


Fig. 6. POD in comparison: MSSR with different inductances (10, 20, and 30 mH).

TABLE IV  
POD TIMES FOR DIFFERENT FAULT TIMES AND LINE OUTAGES

Fault time in ms	line outage	P after fault in MW	$P_{max}$ in MW	$t_{POD}$ in s		No. of switchings
				without MSSR	with MSSR	
80	–	1661	3462	3,02	1,84	2
80	L1	1264	2055	6,78	3,00	3
80	L3	2246	3993	2,11	0,71	1
120	–	1661	4030	4,89	1,84	2
120	L1	1264	2243	10,20	5,22	5
120	L3	2246	4580	3,27	2,30	2

takes only 3 s until the oscillation has died out, which is only half of the time needed before.

1) *Influence of the MSSR Reactance on POD*: Fig. 6 shows the damping of the power oscillation for three different inductances of the inserted MSSR in the base scenario: 10, 20, and 30 mH.

If the inductance is 10 mH, the additional damping is not sufficient and the VCBs have to be switched very often. The oscillation needs at least 4.6 s to get into the 5% range. The situation is improved considerably by choosing an inductance of 30 mH. Now the 5% limits are reached within 2.5 s and there are only two switching operations. But this inductance value is too high if the power oscillation amplitude is lower. This can be the case if other fault types or shorter fault times occur. It was figured out within this investigation that the MSSR with 30 mH could not be inserted in many of these simulated cases, because it would have had a negative influence on the power oscillation damping performance. A compromise between an enhanced operative range and sufficient damping is reached by an inductance of 20 mH, according to the base scenario.

2) *POD for Different Fault Types and Times*: Table IV gives an overview over the times needed so that a power oscillation gets within the 5% limits for different fault times and line outages with and without the MSSR. The fault type changes only the amplitude of the power oscillation and has therefore the same effect as the fault time, so a three-phase grounded fault is always assumed.

The POD always takes less time if the MSSR is utilized. In case of line 3 outage, the MSSR is overloaded by 30%. That is no problem for approximately 10 min because the considered VCBs are able to carry 1.5 times their rated current which is

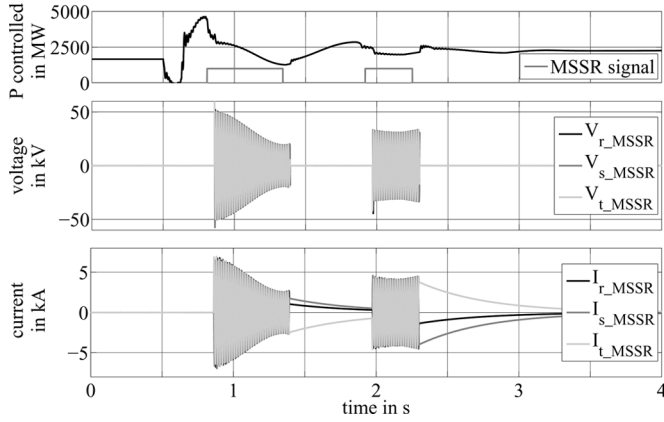
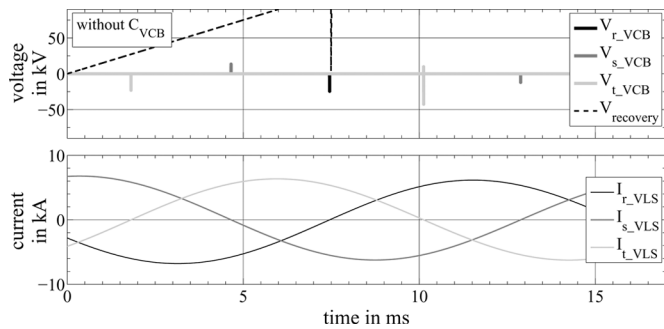


Fig. 7. Voltages and currents of the MSSR.

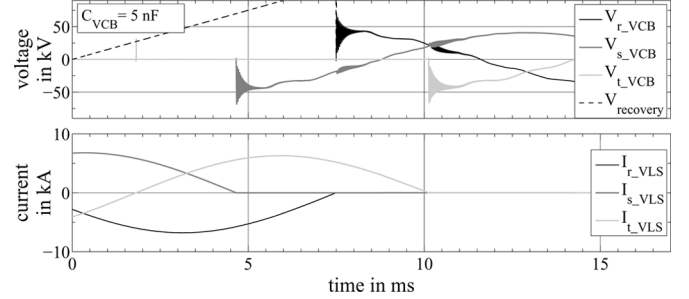
Fig. 8. Detailed TRV across the opening VCB (without  $C_{VCB}$ ).

3.75 kA within this time. If it takes longer to reconfigure the electrical network, the transmitted power has to be reduced.

3) *Currents and Voltages of the VCBs and the Reactor:* In this section, the electrical stress on the components of the MSSR in the base scenario is assessed. The inductance of the MSSR is in this case 20 mH. The most critical case with a 120-ms three-phase fault and line 3 outage is used therefore. A capacitor with 10 nF is switched in parallel to the VCBs as a protective circuit in order to decrease the slope of the transient recovery voltage (TRV). This is described further in Section IV-A.4. A current of 2.42 kA flows through the two VCBs, which short circuit the reactor in steady-state operation before the fault occurs. If one of them is opened, the current is shifted to the reactor. This can be seen in the lower graph of Fig. 7.

Every time the MSSR is short circuited again, a dc-trapped current occurs, which decays with a time constant of  $\tau = R_{mssr}/L_{mssr} = 0.48$  s. When the respective VCB opens the first time, the maximum TRV amplitude across it is 75.7 kV at approximately 0.8 s. The maximum current amplitude of the reactor of the MSSR is 6.85 kA. The VCB currents can reach higher amplitudes up to 9.5 kA when the MSSR is short-circuited again because of the superposition of the DC-trapped current and the line current. All current and voltage amplitudes are within the parameters of the used VCBs.

4) *Stray Capacitances of the MSSR:* The stray capacitances of the MSSR to ground can have a negative effect on the switching capability of the VCBs. Fig. 8 shows the detailed TRV across the opening VCB when the MSSR is inserted as well as the dielectric recovery of the gap.

Fig. 9. Detailed TRV across the opening VCB ( $C_{VCB} = 5$  nF).

Although the maximum voltage of the VCB is not exceeded, a current interruption is impossible because the slope of the TRV is about  $22$  kV/ $\mu$ s, much higher than what the VCBs are able to handle ( $5$  kV/ $\mu$ s, see Table III). This leads to restrikes in the VCBs in all phases, which can be seen when there are spikes at the moments of the current zero crossings in every phase. The current cannot be successfully interrupted. A possibility to avoid transients at the VCBs with high amplitudes and large slopes is to connect a capacitor in parallel to each VCB. This effect can be seen in Fig. 9.

The capacitors across the VCBs have 5 nF and the situation is enhanced considerably. The slope of the TRV is now lower than  $5$  kV/ $\mu$ s and the amplitude is 70 kV both within the VCB parameters. The frequency of the oscillation is approximately 29.7 kHz. In order to maintain a higher safety margin to the VCB specifications, the capacitances in parallel to the VCBs are set to 10 nF for all of the cases previously mentioned.

## B. MSD

The electrical stress on the VCBs is a high TRV when disconnecting the MSCs from the grid and a high inrush current when connecting them. When disconnecting the MSR, a high TRV amplitude, because of the stray capacitances, is expected. The first part of this section shows the simulation result of a scenario while switching the MSCs/MSR, and the second part shows the results of scenario b. A capacitor of 5 nF is connected in parallel to each VCB of the MSCs in order to reduce the slope of the TRV. Regarding the MSR, an RC circuit for protective reasons is used, which is explained at the end of the following subsection.

1) *Electrical Stress Voltages (Scenario a):* The simulation is started with an increased load so the voltage drops to 392 kV. One MSC is connected to the node in order to maintain a node voltage of 400 kV. After steady-state conditions are attained, the load is decreased to the original value of 100% which leads to a voltage increase to approximately 408 kV. The MSC is finally disconnected whereas the moment of disconnecting it is varied over one period of power system frequency. The maximum occurring TRV amplitude is recorded. Fig. 10 shows the voltage and current of the VCB and the capacitor voltage while the MSC is disconnected.

The lower graph shows that the capacitor voltages remain constant immediately after the current is interrupted. They decrease with the time constant of 18 s calculated before. In [23], it is specified that the capacitor voltage should be lower than 50 V

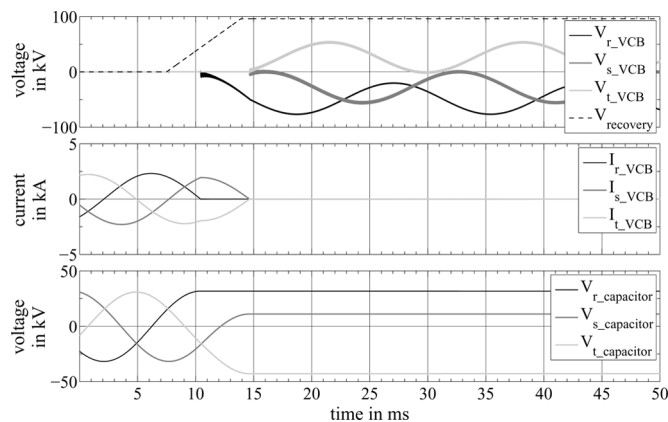


Fig. 10. Voltages and currents while disconnecting an MSC.

TABLE V  
VOLTAGES WHILE DISCONNECTING ONE MSC

MSCs in service	$V_{\text{transf\_rms}}$ in kV		$ V_{\text{VCB\_max}} $ in kV	$ V_{\text{capacitor\_max}} $ in kV
	before disconnecting	after		
1	36.1	34.1	77.5	42.8
2	37.7	35.4	81.1	44.7
3	39.4	36.9	84.5	46.7

after 5 min. Assuming an initial voltage of 50 kV, it takes about 2 min until 50 V are obtained so that is within the requirement.

The same sequence is repeated but two/three MSCs are connected to the load node before disconnecting one MSC in order to keep the voltage at 400 kV. Table V shows the voltages on the LV side of the transformer before and after disconnecting one MSC, the maximum voltage of the opening VCB, and the maximum capacitor voltage.

Regarding these three cases, the capacitive voltage rise leads to high TRV values in the first interrupting phase, but all values are within the VCB specifications.

In the next investigated case, all three MSCs are connected to the node because of a heavy load in order to obtain a node voltage of 400 kV. After a strong load reduction, all MSCs have to be disconnected from the node as quickly as possible in order to avoid an overvoltage at the load node. The earliest moment of disconnecting them is set to 80 ms. This time composes a time delay because of the properties of the VCBs and for detecting the overvoltage. The first MSC is disconnected in the voltage maximum, and the switching moments of the other MSCs are varied within a period of power system frequency. The maximum voltage of 87.1 kV is detected in the second disconnected MSC when it is disconnected 0.5 ms after the first and third MSC. This value is close to 96 kV given in Table III. In order to maintain a higher safety margin, it is possible to use a grounded capacitor bank and a transformer with a grounded star connection on the LV side. Then, the theoretical maximum voltage across the VCBs is twice the amplitude of the MSC voltage [18].

The maximum voltage while disconnecting the MSR is assessed now. A TRV with a high amplitude can occur because of the stray capacitances to ground. An RC circuit with  $R = 200 \Omega$  and  $C = 20 \text{ nF}$  is placed from the terminal of the reactor that is

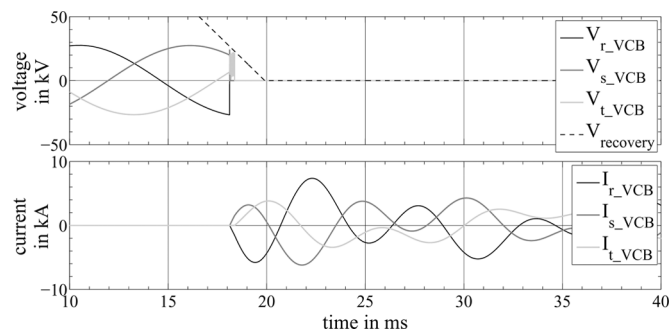


Fig. 11. Voltages and currents while connecting an MSC.

connected to the VCB to ground in order to avoid TRV slopes that the VCB is not able to handle. The simulation starts with a high load and all MSCs are connected. The node voltage is 400 kV. Now the load is decreased so that only the MSR has to be disconnected. The maximum recorded voltage while varying the time of disconnecting it is 87.7 kV, which is within the parameter of the used VCB.

2) *Electrical Stress—Currents (Scenario a)*: At first the currents during single bank switching are investigated and afterwards the currents during back to back switching. The simulation is started with 100% load followed by an load increase. The voltage drops to 392 kV and one MSC has to be connected in order to obtain 400 kV. The moment of switching is varied over one period of power system frequency and the maximum current of the VCB recorded but only while it is closing: with closed contacts, the VCB is able to handle currents up to 100 kA for a few seconds [14]. Fig. 11 shows the VCB currents and voltages while the MSC is connected.

The inrush current gets maximal if the respective capacitor of the MSC is connected in the voltage maximum. In this case, phase r has a voltage maximum, while the capacitor is connected so the current in the same phase reaches its maximum value of 5.8 kA within the closing process. The closing process can be seen in the upper graph, while the dielectric recovery of the VCB decreases to zero. The maximum current after the finished closing process is 7.6 kA. The current amplitude in this case is mainly influenced by the voltage amplitude, the inductances in the source path (source, line, transformer, current limiting reactor), and the capacitance of the MSC. Although the resonant circuit of current limiting reactor and the capacitance is designed to the fourth harmonic, the frequency of the current oscillation is 173 Hz, which is considerably lower. This is due to the inductance of the source path in case of single-bank switching. The ohmic part of the load causes a fast decrease of the higher harmonics in the current.

Now, the same situation is investigated, but this time, the connected MSC has precharged capacitors. That means, it has been disconnected some seconds before and, for some reasons, has to be connected again. The capacitor which has the highest voltage difference to the system voltage, while being connected again, generates the highest current amplitude. The moment of connecting the MSC again is varied and the maximum recorded current amplitude within the closing process is 14.2 kA. The capacitor voltages attain high values up to 81 kV because of the high currents.

Since the aforementioned case with a precharged MSC results in much higher currents, this case is applied for the investigation of back-to-back switching. The simulation starts with all MSCs connected because of a high load. One MSC is disconnected and shortly thereafter, it is connected again. The maximum current amplitude is now 17.5 kA, which is relatively close to limit given in [16]. The currents in the other MSCs are reaching values up to 12.7 kA, but that is no problem since the VCBs are closed. The maximum recorded capacitor voltage is 99 kV. The currents now are mainly influenced by the inductances between the MSCs and not by the inductances in the source path as in the case of single-bank switching. Now the frequency of the higher harmonic current is approximately 240 Hz as expected. The current oscillations are only damped by the losses of the capacitors and the limiting reactors in this case which takes longer than during single-bank switching. The current amplitudes do not increase very much if one or two MSCs are already connected while another precharged MSC is connected too. This is because the inductances of the source path and the inductance of the current limiting reactors are within a similar range. This can be seen if the inrush current frequency is regarded. It is 173 Hz for single-bank switching and 240 Hz for back-to-back switching. A slight current rise can be determined mainly because of the capacitive voltage rise, which is increasing as more MSCs are connected.

3) *Scenario b*: Now the results of scenario b are presented where the load consists of 70% induction machines. In the first case, the system is running in steady state. The machines are running with a rated speed of 0.98 p.u. and the active power of the total load is nearly 1000 MW. An additional moment of inertia is considered at the shaft of the induction machines so that a total inertia constant of  $H = 2.84$  s results. The exponent of the load shaft is set to zero. This is the worst case scenario as the mechanical load requires a constant torque, independent of the machines speed. A PD controller serves to connect and disconnect the MSCs at the right time. It uses the difference of the node voltage to the desired value of 400 kV as an input signal, and the output is the required reactive power. Fig. 12 shows the power of the induction machines, the effective voltage on the LV side of the transformer (middle graph), and the speed of the machines (lower graph) for a 120-ms three-phase fault with a ground connection at point F (see Fig. 4). In one case, the MSD is in service; in the other case, it is not. The dashed lines show the last case.

The fault occurs at 0.4 s. During the fault, the voltage drops strongly which can be seen in the middle graph. After it has been cleared, the reactive power consumption is increased from 350 to 650 Mvar and the active power from 700 to 870 MW. The decrease of the machines speed can be seen in the lower graph. All MSCs are connected as soon as the fault is detected. This is after 51 ms, which includes the time delay of the VCBs. The rated speed is achieved again after 1.82 s. The moments of disconnecting the three MSCs can be seen in the middle graph when there are spikes in the voltage curve. Without connecting the MSCs, the reactive power consumption remains higher and the speed decreases continuously. The voltage drops further and a voltage collapse cannot be avoided.

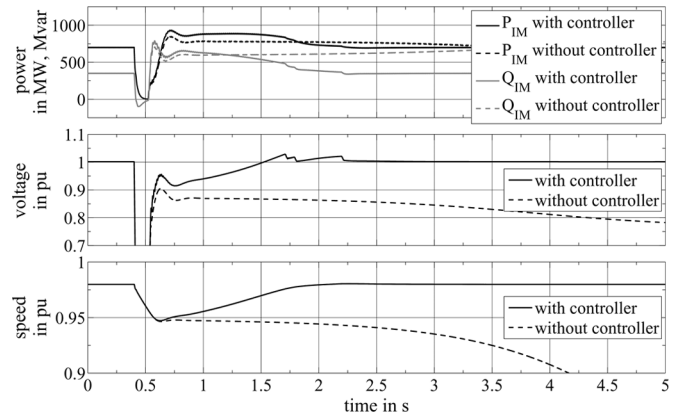


Fig. 12. Voltage and speed of IM after the fault with and without the controller.

TABLE VI  
TIME UNTIL RATED VOLTAGE IS ACHIEVED AGAIN  
AFTER A FAULT (1\* SYSTEM GETS UNSTABLE)

fault type	fault time in ms	time in s		$\Delta$ time in %
		without MSCs	with MSCs	
1-phase, ground	80	1,92	0,92	52
2-phase	80	2,28	1,02	55
3-phase, ground	80	3,30	1,41	57
1-phase, ground	120	2,30	1,07	53
2-phase	120	2,86	1,31	54
3-phase, ground	120	1*	1,82	–

Table VI shows the times until the rated voltage is achieved again at the load node if the MSCs are connected and if they are not connected. Three different fault types are investigated and two different fault times.

The time until the rated voltage is achieved again can be cut into halves in all considered cases. Further simulations with different fault types showed that the fault times can be increased by the half without leading to a voltage collapse if the MSCs are used.

It is not possible for the three MSCs to be connected at the same moment in reality due to switching delays caused by the differing mechanical properties of the VCBs. There will be rather a short time delay. The switching moments of all MSCs are varied over one period of power system frequency and the maximum current amplitudes are recorded. The highest value while the VCBs are closing occurs in the last connected MSC and is 7.5 kA. All simulations did not show exceeded maximum tolerable currents during the closing process of the VCBs. The maximum voltage across the VCBs, when the MSCs are disconnected, does not exceed the parameter of the used VCBs because it is disconnected consecutively as the voltage at the load node reaches the desired value comparatively slow.

## V. CONCLUSION

This paper shows that the utilization of VCBs in FACTS is promising in investigated applications—the MSSR and the MSD. The MSSR can support a TCSC in order to maintain better performance for power oscillation damping by enhancing

the inductive range of the TCSC. The time until the power oscillation reaches a satisfactory value could be reduced up to the half in the investigated cases as if only the TCSC was used. The time delays of the VCBs do not have a negative influence on POD as they can be compensated by adapting the threshold values for inserting and removing the MSSR. A capacitor is necessary in parallel to the VCBs in order to reduce the slope of the TRV, which occurs while opening. With this protective circuit, the resulting electrical stress on the VCBs while switching operations occur does not exceed their parameters.

Regarding the MSD, this paper shows that it is able to stabilize the voltage at a load node and to avoid a voltage collapse although the VCBs have time delays because of their mechanical properties. Either the fault time can be increased without leading to a voltage collapse or the time can be reduced until the voltage achieves the desired value after a fault at the load node. All investigated cases show that mainly TRV with high amplitudes and slopes occurs across the VCBs while they are opening, and high-current amplitudes occur while they are closing. By using protective circuits, such as the capacitors across the VCBs of the MSCs and the RC-circuit of the MSR, the parameters of the selected VCBs are not exceeded. Current-limiting reactors are utilized further in order to limit the inrush currents.

#### REFERENCES

- [1] L. Aengquist, "Synchronous voltage reversal control of thyristor controlled series capacitor," Ph.D. dissertation, Royal Inst. Technol., Stockholm, Sweden, 2002.
- [2] M. R. Sharp, R. G. Andrei, and J. C. Werner, "A novel air-core reactor design to limit the loading of a high voltage interconnection transformer bank," in *Proc. IEEE Power Eng. Soc. Summer Meeting*, Jul. 2002, vol. 1, pp. 494–499.
- [3] D. Shoup, J. Paserba, R. G. Colclaser, T. Rosenberger, L. Ganatra, and C. Isaac, "Transient recovery voltage requirements associated with the application of current-limiting series reactors," in *Proc. Int. Conf. Power Syst. Transients*, Jun. 2005, pp. 1–6.
- [4] A. Carrus, E. Cinieri, and F. M. Gatta, "Improving the security of sub-transmission systems by use of temporary insertion of series and shunt reactances," presented at the IEEE Power Tech. Conf., Bologna, Italy, Jun. 2003.
- [5] G. Wolf, J. Skliutas, G. Drobnyak, and M. D. Costa, "Alternative method of power flow control using air core series reactors," in *Proc. IEEE Power Eng. Soc. Gen. Meeting*, Jul. 2003, vol. 2, pp. 574–580.
- [6] CIGRE, Task Force 38.01.06, "Load flow control in high voltage power systems using FACTS controllers," CIGRE Tech. Brochure 51, 1996.
- [7] H. Weber, "Ursachen von netzpendelungen," *VDI-Bericht 1329, 4. GMA/ETG-Fachtagung Netzregelung, VDI/VDE-Tagung Berlin*, 1997.
- [8] R. M. Mathur and R. K. Varma, *Thyristor-Based FACTS Controllers for Electrical Transmission Systems*. Piscataway, NJ: IEEE, 2002.
- [9] *Flexible AC Transmission Systems*, Y. H. Song and A. T. Johns, Eds. London, U.K.: Inst. Elect. Eng., 1999.

- [10] T. Van Cutsem and C. Vournas, *Voltage Stability of Electric Power Systems*. Norwell, MA: Kluwer, 1998.
- [11] M. Z. El-Sadek and F. N. Abdelbar, "Effects of induction motor load in provoking transient voltage instabilities in power systems," *Elect. Power Syst. Res.*, vol. 17, p. 119127, 1989.
- [12] H.-J. Lippmann, *Schalten im Vakuum—Physik und Technik der Vakuumschalter*. Berlin, Germany: VDE Verlag GmbH, 2003.
- [13] Vakuum-Schaltechnik und Komponenten fuer die Mittelspannung Catalogue HG 11.01, Siemens AG, 2007.
- [14] Vakuum-Leistungsschalter 3AH4, Mittelspannungsgeraete, Auswahl- und Bestelldaten Catalogue HG 11.04, Siemens AG, 2008.
- [15] *Handbook of Switchgears*. New York: McGraw-Hill, 2007.
- [16] *IEEE Standard for AC High-Voltage Circuit Breakers Rated on a Symmetrical Current Basis—Preferred Ratings and Related Required Capabilities for Voltages Above 1000 V*, IEEE Standard C37.06, 2009.
- [17] A. D. Del Rosso, C. A. Cañizares, and V. M. Doña, "A study of tcsc controller design for power system stability improvement," *IEEE Trans. Power Syst.*, vol. 18, no. 4, pp. 1487–1496, Nov. 2003.
- [18] O. Oeding and B. R. Oswald, *Elektrische Kraftwerke und Netze*, 6th ed. Berlin, Germany: Springer-Verlag, 2004.
- [19] PSCAD—Electromagnetic Transients, Users Guide Manitoba HVDC Research Centre Inc. Winnipeg, MB, Canada, 2005.
- [20] P. Kundur, *Power System Stability and Control*. New York: McGraw-Hill, 1994.
- [21] Schorch, Jan. 2010, Drehstrom—Asynchronmotoren fuer hochspannung. Datasheet KA2569XBH04G, Schorch Elektrische Maschinen und Antriebe GmbH. [Online]. Available: <http://www.schorch.de>
- [22] T. Wenzel, T. Leibfried, and D. Retzmann, "Dynamical simulation of a vacuum switch with PSCAD," presented at the 16th Power Syst. Comput. Conf., Glasgow, U.K., Jul. 2008.
- [23] *IEEE Standard for Shunt Power Capacitors*, IEEE Standard 18, 2002.



**Timo Wenzel** received the Diploma degree in electrical engineering from the University of Karlsruhe, Karlsruhe, Germany, in 2006.

Since 2006, he has been with the Institute of Electric Energy Systems and High-Voltage Technology, Karlsruhe Institute of Technology, Karlsruhe. His research interests include vacuum circuit breakers, flexible ac transmission systems, and voltage quality. In 2011, he successfully completed his Ph.D. dissertation on the application of vacuum circuit breakers in flexible ac transmission systems.



**Thomas Leibfried** (M'11) was born in Neckarsulm, Germany, in 1964. He received the Dipl.-Ing. and Dr.-Ing. degrees from the University of Stuttgart, Stuttgart, Germany, in 1990 and 1996, respectively.

From 1996 to 2002, he was with Siemens AG, working in the power transformer business in various technical and management positions. In 2002, he joined the University of Karlsruhe (now Karlsruhe Institute of Technology, KIT) as Head of the Institute of Electric Energy Systems and High-Voltage Technology.

Prof. Leibfried is a member of VDE and CIGRE and the author of many technical papers.